

Retinal Image Restoration using Transformer and Cycle-Consistent Generative Adversarial Network

Alnur Alimanov

Department of Computer Engineering
Bahcesehir University, Istanbul, Turkey
Email: alnur.alimanov@bahcesehir.edu.tr

Md Baharul Islam

Bahcesehir University, Istanbul, Turkey
American University of Malta
ORCID: 0000-0002-9928-5776

Abstract—Medical imaging plays a significant role in detecting and treating various diseases. However, these images often happen to be of too poor quality, leading to decreased efficiency, extra expenses, and even incorrect diagnoses. Therefore, we propose a retinal image enhancement method using a vision transformer and convolutional neural network. It builds a cycle-consistent generative adversarial network that relies on unpaired datasets. It consists of two generators that translate images from one domain to another (e.g., low- to high-quality and vice versa), playing an adversarial game with two discriminators. Generators produce indistinguishable images for discriminators that predict the original images from generated ones. Generators are a combination of vision transformer (ViT) encoder and convolutional neural network (CNN) decoder. Discriminators include traditional CNN encoders. The resulting improved images have been tested quantitatively using such evaluation metrics as peak signal-to-noise ratio (PSNR), structural similarity index measure (SSIM), and qualitatively, i.e., vessel segmentation. The proposed method successfully reduces the adverse effects of blurring, noise, illumination disturbances, and color distortions while significantly preserving structural and color information. Experimental results show the superiority of the proposed method. Our testing PSNR is 31.138 dB for the first and 27.798 dB for the second dataset. Testing SSIM is 0.919 and 0.904, respectively. The code is available at <https://github.com/AAleka/Transformer-Cycle-GAN>

Index Terms—Retinal image restoration, deep learning, transformer, generative adversarial network.

I. INTRODUCTION

The retina of the central nervous system is responsible for transforming the incoming light into a neural signal and sending it to the brain's visual cortex for processing. Therefore, ophthalmologists can diagnose eye, brain, and blood circulation diseases by analyzing the retinal images. However, sometimes due to poor imaging device configuration, misoperations during the imaging process, and patient restlessness (primarily applicable to children), these images suffer from such degradation types as out-of-focus blurring, image noise, low, high, and uneven illuminations, and color distortion. It suffers a tremendous negative impact on treatment efficiency, the extra time and money expenditure, and even misdiagnosis.

In recent years, deep learning-based techniques [1]–[3] are used to detect and classify diseases using retinal images. However, these methods rely on high-quality images during analysis, which is not always possible to acquire in some cases. Researchers also propose traditional methods [4], [5] to enhance these images. However, they often suffer from

generalization issues, meaning they cannot be applied to all cases. For example, Zhang et al. [5], took the reflective feature of the fundus camera into account. They proposed a double-pass fundus reflection model (DPFR) that improves the contrast of retinal images. However, the presence of image artifacts is noticeable. Many learning-based techniques [6]–[11] have been introduced to solve this problem. However, most of these works solved the missing paired data problem by manually degrading original high-quality fundus images. Manually degraded images are different from original low-quality retinal images. Thus, these methods show poor performance when enhancing real degradation effects. For instance, the authors of [11] developed a restoration deep learning network that was trained using simulated cataract-like images. However, it performs worse when it comes to restoring real low-quality images.

This paper introduces a novel deep learning retinal image restoration model based on a cycle-consistent generative adversarial network with modified generators that do not require paired datasets. Our model replaced the traditional CNN encoder with a vision transformer encoder, resulting in faster convergence, superior quantitative and qualitative outcomes, and better structural and color preservation than other methods. The method has been trained and validated using two publicly available datasets [12], [13]. The contributions can be summarized as follows:

- We propose a novel CycleGAN architecture consisting of a vision transformer and convolutional neural network. To the best of our knowledge, this is the first attempt to combine CNN with a transformer in CycleGAN architecture.
- Replacing the transformer decoder with a CNN decoder reduced the computational expense compared to pure transformer CycleGAN architecture, which allowed us to use a large image size.

II. METHODOLOGY

A. Model Architecture

Our method is based on CycleGAN, initially proposed by [14]. However, we replaced the CNN encoder in the generator network with a vision transformer encoder, as shown in Fig. 1. Using CNN as a decoder decreased computational expenses compared to a pure transformer network which allowed

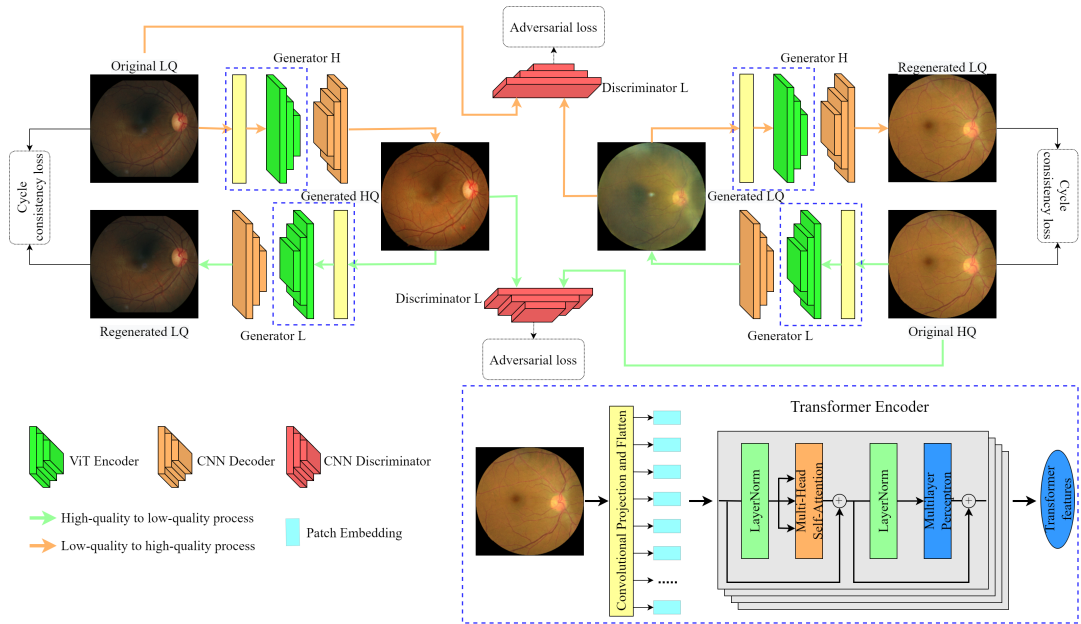


Fig. 1. The workflow of the proposed method. Low-quality images go through Generator H and the result - Generated HQ - is inputted into Generator H and Discriminator H. Next, the Generated LQ image is made from high-quality image using Generator L, then this generated image is passed to both Generator H and Discriminator L. After these steps, losses are calculated.

to increase the image size by a factor of 4, from 64×64 to 256×256 . This network consists of a pair of generator networks (G_H and G_L) and a pair of discriminators (D_H and D_L). The task of each generator is to translate images from one domain to another and to fool the corresponding discriminator. For instance, G_H is trying to generate realistic, high-quality images from original low-quality ones, and D_H receives this generated image and one original high-quality image and calculates the probability of a given image being authentic. As a result, generators and discriminators are playing an adversarial game.

A discriminator is a CNN-based classifier that consists of such layers as 2D convolution, LeakyReLU activation function, and instance normalization. Firstly, a colorful 256×256 image is fed into the convolutional layer with output channels, kernels size, stride, and padding equal to 64, 4, 2, and 1, respectively. Then, we used the LeakyReLU activation function. The result sends to three consecutive downsampling blocks: convolutional layer, instance normalization, and LeakyReLU. Kernel size and padding are equal to 4 and 1, but output features double after each downsampling process starting from 64 and ending with 512. Stride is 1 in the first and 2 in the last two blocks. In the end, it is fed into the final convolutional layer with output channel, stride, and padding equal to 1 and kernel size being 4. As a result, we get a 30×30 patch and make predictions using the sigmoid activation function.

The generator consists of a vision transformer encoder and a CNN decoder. Firstly, each input image of size 256×256 is divided into patches of size 8×8 using a convolutional projection proposed by [15]. It provides additional efficiency. Instead of a depth-wise convolutional layer with batch normal-

ization, we only used a convolutional layer with 1024 output channels, kernel, and stride sizes of 1. Then we flattened the 3D output to 2D and transposed it. It reduced the computation time without affecting the accuracy of the method. Then these flattened sequences are fed into a standard transformer encoder network as shown in Fig. 1. Our network's depth and projection dimensions are 7 and 1024, respectively. The output shape of this encoder is 1024×1024 . Therefore, we reshaped it into $1024 \times 32 \times 32$ to feed into the CNN decoder. It consists of 3 upsampling blocks: transpose convolution, instance normalization, and ReLU activation function. The output channels have been decreased by 2 after each block; kernel size, stride, padding, and output padding in all blocks are 3, 2, 1, and 1, respectively. The resulted matrix of shape $128 \times 256 \times 256$ is converted into a color image using the last convolutional layer with a kernel size of 7, the stride of 1, and padding of 3. The final output is activated using a hyperbolic tangent.

B. Loss functions

1) *Adversarial Loss*: Adversarial loss has been developed in the first GAN work [16] that can be formulated as discriminator loss. Given low-quality image L , high-quality image H , a generator G_H that transforms L to high quality \hat{H} , G_L that degrades images (from Y to \hat{X}), D_H and D_L classify high- (H , \hat{H}) and low-quality images (L and \hat{L}), respectively. Mathematically, this loss function is expressed as follows:

$$\begin{aligned}
 L_A(D_L, L, \hat{L}) &= E_L[\log(D_L(L))] + E_{\hat{L}}[\log(1 - D_L(\hat{L}))] \\
 L_A(D_H, H, \hat{H}) &= E_H[\log(D_H(H))] + E_{\hat{H}}[\log(1 - D_H(\hat{H}))]
 \end{aligned}
 \tag{1}$$

2) *Cycle Consistency Loss*: Cycle-consistency can be formulated as follows: a generated image \hat{H} translated back to \hat{L} should not be different from L . The same things apply for H and a regenerated \hat{H} from \hat{L} . The difference between regenerated and original images is calculated using the $L1$ function in the following way:

$$\begin{aligned} L_C(\hat{L}, L) &= E_L[||\hat{L} - L||_1] \\ L_C(\hat{H}, H) &= E_H[||\hat{H} - H||_1] \end{aligned} \quad (2)$$

3) *Identity loss*: To calculate identity loss, we use generators and images from the same domains. More specifically, H should not be modified when it is sent to G_H . The same things apply to L and G_L . To calculate this loss function, we also use the $L1$ function in the following way:

$$\begin{aligned} L_I(L, G_L(L)) &= E_L[||L - G_L(L)||_1] \\ L_I(H, G_H(H)) &= E_H[||H - G_H(H)||_1] \end{aligned} \quad (3)$$

4) *Total loss*: The total generator and discriminator loss can be formulated as:

$$\begin{aligned} L(G_L, G_H, D_L, D_H) &= L_A(D_L, L, \hat{L}) + L_A(D_H, H, \hat{H}) + \\ &+ \lambda_1 L_C(\hat{L}, \hat{L}) + \lambda_1 L_C(\hat{H}, \hat{H}) + \\ &+ \lambda_2 L_I(L, G_L(L)) + \lambda_2 L_I(H, G_H(H)) \end{aligned} \quad (4)$$

where λ_1 and λ_2 are weights of cycle consistency and identity losses. The main problem that discriminators and generators are trying to solve can be mathematically expressed in the following equation:

$$G_L^*, G_H^* = \arg \min_{G_L, G_H} \max_{D_L, D_H} L(G_L, G_H, D_L, D_H) \quad (5)$$

III. RESULTS AND DISCUSSION

A. Datasets

In our work, we used two datasets, such as EyeQ [12] and Mendeley [13]. EyeQ dataset has 16818 "Good", 6434 "Usable", and 5,538 "Bad" images of size 800×800 . The Mendeley dataset comprises 1146 "Artifacts" and 1060 "No artifacts" images of size 350×346 . For training, we used all "Good," "No artifacts," 5455 "Usable," and 986 "Artifacts" images. The testing set includes 979 "Usable" and 160 "Artifacts" images. To train vessel segmentation model, we used DRIVE [17] dataset that includes 40 images of size 565×584 with corresponding manually annotated segmentation's.

B. Experimental Setup

We implement the proposed model in the PyTorch framework. The hardware configurations are Intel Core i7-10700f CPU, 32 GB of RAM, and an NVIDIA GeForce RTX 2080 SUPER 8 GB. The model was set to train for 100 epochs with early stopping as soon as average generator loss stops decreasing. The generator loss has decreased, while discriminator loss has increased for 23 epochs. The generator model improved faster than the discriminator until both converged. The total training time is 25 hours for our experiment.

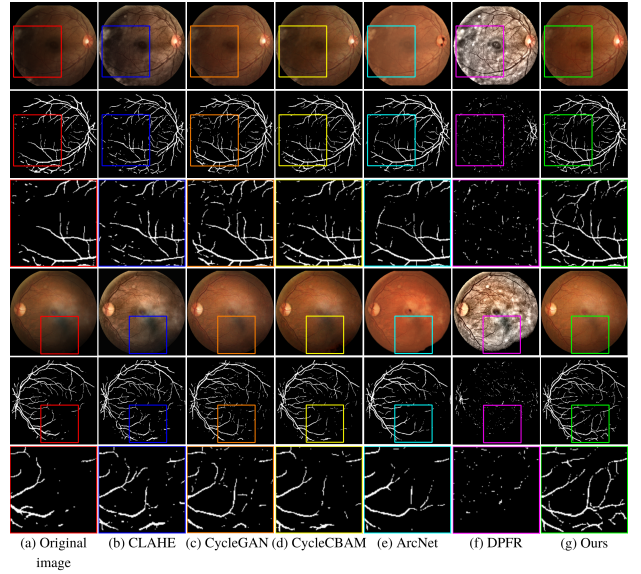


Fig. 2. Comparison with state-of-the-art methods. From top to bottom are fundus image, corresponding segmentation and zoomed segmentation. (a) low-quality image, (b) CLAHE [4], (c) CycleGAN [6], (d) CycleCBAM [10], (e) ArcNet [11], (f) DPFR [5], (g) Ours.

C. Qualitative and Quantitative Performance

To validate the efficiency of our method, we performed qualitative analysis for restored images using vessel segmentation with 5 state-of-the-art methods: CLAHE [4], CycleGAN [6], Cycle-CBAM [10], ArcNet [11], DPFR [5]. UNet [18] was trained using pairs of fundus images with corresponding manually segmented images from DRIVE dataset [17]. Fig. 2 shows the restoration and vessel segmentation results. Our method enhanced the retinal image better compared to the state-of-the-art. In addition, our result has less noise compared to CycleGAN [6] and CycleCBAM [10]. Algorithm-based methods [4], [5] could improve the contrast making vessels visible, but produced images have artifacts. ArcNet [11] failed to restore tiny blood vessels in the dark region.

To further evaluate our results, we conducted the quantitative analysis with the same methods. The evaluation metrics include PSNR, SSIM, and single image test time (SITT), as shown in TABLE I. As we can see, our method significantly outperforms all other methods in terms of PSNR and SSIM with the EyeQ dataset. Our approach also shows the best results compared to the state-of-the-art for the Mendeley dataset. In terms of SITT, it shows competitive outcomes taking the third position after CLAHE [4] and original CycleGAN [6].

D. Ablation study

To conduct an ablation study of our work, we trained and tested the original fully convolutional CycleGAN model with the same datasets. Total training time for the traditional CycleGAN required 40 hours to converge, 15 hours more than ours. Additionally, testing PSNR values of our and traditional methods are 31.138 dB and 25.577 dB for the EyeQ dataset, and for the Mendeley dataset, the values are 27.798 dB and

TABLE I
COMPARISON WITH STATE-OF-THE-ART METHODS.

Dataset	Method	PSNR	SSIM	SITT
EyeQ [12]	CLAHE [4]	25.152 dB	0.716	17ms
	CycleGAN [6]	25.577 dB	0.882	90ms
	Cycle-CBAM [10]	26.263 dB	0.901	100ms
	ArcNet [11]	21.073 dB	0.87	183ms
	DPFR [5]	12.423 dB	0.34	449ms
	Ours	31.138 dB	0.919	97ms
Mendeley [13]	CLAHE [4]	26.07 dB	0.77	17ms
	CycleGAN [6]	26.08 dB	0.9	90ms
	Cycle-CBAM [10]	25.808 dB	0.901	100ms
	ArcNet [11]	22.17 dB	0.891	183ms
	DPFR [5]	12.797 dB	0.304	449ms
	Ours	27.798 dB	0.904	97ms

26.08 dB, respectively. The SSIM values are 0.919 and 0.882 for the EyeQ and 0.904 and 0.9 for the Mendeley datasets, respectively. On average, testing one image takes 90ms for CNN CycleGAN and 97ms for our method, meaning that our modification did not add much computational expense. Fig. 3 demonstrates the qualitative comparison of these two methods. Our method is better at restoring tiny, barely visible blood vessels and preserving structural and color information of original images.

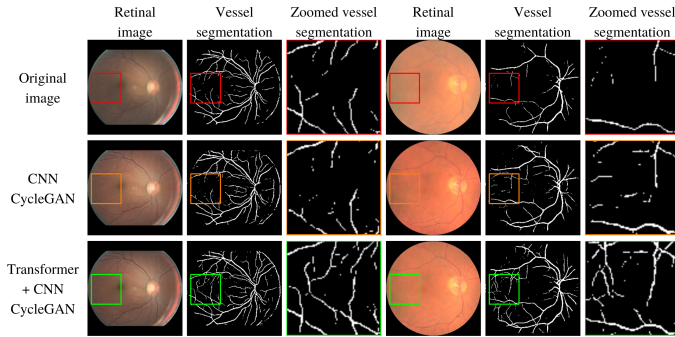


Fig. 3. Qualitative comparison of tiny blood vessels restoration.

IV. CONCLUSION

In this paper, we combined a vision transformer and convolutional neural network, resulting in better retinal image enhancement than fully convolutional CycleGAN and other state-of-the-art techniques. In addition, our goal was to reduce the computational expense of transformer CycleGAN architecture without compromising the performance. This simple yet effective combination has led to comparatively better quantitatively, qualitatively, and computational performance. The model was tested using two datasets, such as EyeQ [12] and Mendeley dataset [13]. Testing PSNR is 31.138 dB for the first and 27.798 dB for the second dataset. Testing SSIM is

0.919 and 0.904, respectively. The ablation study demonstrates a significant advantage of our method compared to the original CycleGAN architecture.

REFERENCES

- [1] F. Grassmann, J. Mengelkamp, C. Brandl, S. Harsch, M. E. Zimmermann, B. Linkohr, A. Peters, I. M. Heid, C. Palm, and B. H. Weber, "A deep learning algorithm for prediction of age-related eye disease study severity scale for age-related macular degeneration from color fundus photography," *Ophthalmology*, vol. 125, no. 9, pp. 1410–1420, 2018.
- [2] Z. Gao, J. Li, J. Guo, Y. Chen, Z. Yi, and J. Zhong, "Diagnosis of diabetic retinopathy using deep neural networks," *IEEE Access*, vol. 7, pp. 3360–3370, 2018.
- [3] Y. Peng, S. Dharssi, Q. Chen, T. D. Keenan, E. Agrón, W. T. Wong, E. Y. Chew, and Z. Lu, "Deepseenet: a deep learning model for automated classification of patient-based age-related macular degeneration severity from color fundus photographs," *Ophthalmology*, vol. 126, no. 4, pp. 565–575, 2019.
- [4] F. M. Shamsudeen and G. Raju, "Enhancement of fundus imagery," in *2016 International Conference on Next Generation Intelligent Systems (ICNGIS)*. IEEE, 2016, pp. 1–5.
- [5] S. Zhang, C. A. Webers, and T. T. Berendschot, "A double-pass fundus reflection model for efficient single retinal image enhancement," *Signal Processing*, vol. 192, p. 108400, 2022.
- [6] Q. You, C. Wan, J. Sun, J. Shen, H. Ye, and Q. Yu, "Fundus image enhancement method based on cyclegan," in *2019 41st annual international conference of the IEEE engineering in medicine and biology society (EMBC)*. IEEE, 2019, pp. 4500–4503.
- [7] W. Li, G. Liu, Y. He, J. Wang, W. Kong, and G. Shi, "Quality improvement of adaptive optics retinal images using conditional adversarial networks," *Biomedical optics express*, vol. 11, no. 2, pp. 831–849, 2020.
- [8] A. D. Pérez, O. Perdomo, H. Rios, F. Rodríguez, and F. A. González, "A conditional generative adversarial network-based method for eye fundus image quality enhancement," in *International Workshop on Ophthalmic Medical Image Analysis*. Springer, 2020, pp. 185–194.
- [9] A. Alimanov and M. B. Islam, "Retinal image restoration and vessel segmentation using modified cycle-cbam and cbam-unet," 2022.
- [10] C. Wan, X. Zhou, Q. You, J. Sun, J. Shen, S. Zhu, Q. Jiang, and W. Yang, "Retinal image enhancement using cycle-constraint adversarial network," *Frontiers in Medicine*, vol. 8, 2021.
- [11] H. Li, H. Liu, Y. Hu, R. Higashita, Y. Zhao, H. Qi, and J. Liu, "Restoration of cataract fundus images via unsupervised domain adaptation," in *2021 IEEE 18th International Symposium on Biomedical Imaging (ISBI)*. IEEE, 2021, pp. 516–520.
- [12] H. Fu, B. Wang, J. Shen, S. Cui, Y. Xu, J. Liu, and L. Shao, "Evaluation of retinal image quality assessment networks in different color-spaces," in *International Conference on Medical Image Computing and Computer-Assisted Intervention*. Springer, 2019, pp. 48–56.
- [13] T. K. Yoo, J. Y. Choi, and H. K. Kim, "Cyclegan-based deep learning technique for artifact reduction in fundus photography," *Graefes Archive for Clinical and Experimental Ophthalmology*, vol. 258, no. 8, pp. 1631–1637, 2020.
- [14] J.-Y. Zhu, T. Park, P. Isola, and A. A. Efros, "Unpaired image-to-image translation using cycle-consistent adversarial networks," in *Proceedings of the IEEE international conference on computer vision*, 2017, pp. 2223–2232.
- [15] H. Wu, B. Xiao, N. Codella, M. Liu, X. Dai, L. Yuan, and L. Zhang, "Cvt: Introducing convolutions to vision transformers," in *Proceedings of the IEEE/CVF International Conference on Computer Vision*, 2021, pp. 22–31.
- [16] I. Goodfellow, J. Pouget-Abadie, M. Mirza, B. Xu, D. Warde-Farley, S. Ozair, A. Courville, and Y. Bengio, "Generative adversarial nets," *Advances in neural information processing systems*, vol. 27, 2014.
- [17] J. Staal, M. D. Abràmoff, M. Niemeijer, M. A. Viergever, and B. Van Ginneken, "Ridge-based vessel segmentation in color images of the retina," *IEEE transactions on medical imaging*, vol. 23, no. 4, pp. 501–509, 2004.
- [18] O. Ronneberger, P. Fischer, and T. Brox, "U-net: Convolutional networks for biomedical image segmentation," in *International Conference on Medical image computing and computer-assisted intervention*. Springer, 2015, pp. 234–241.